HUMAN BODY'S MICRO-CLIMATE: MEASUREMENT AND SIMULATION FOR THE COUPLING OF CFD WITH A HUMAN THERMOREGULATION MODEL

Conrad Voelker and Oliver Kornadt
Department of Building Physics, Bauhaus-Universität Weimar, Germany

ABSTRACT

When coupling computational fluid dynamics (CFD) with a detailed thermal comfort model describing the human thermoregulation, the characteristics of the micro-climate of the human body have to be known. In the paper, CFD has been applied to investigate human body's micro climate. A climate chamber equipped with a thermal manikin has been used to validate the CFD simulations against measurements for various boundary conditions. Based on the validated simulations, the characteristics of the human micro-climate are analyzed. Finally, an approach for the data exchange of a coupling between CFD and human thermoregulation is introduced.

INTRODUCTION

Estimating the level of thermal comfort is of paramount importance when designing buildings. Unfortunately, the methods commonly used do not take into consideration several fundamental factors as the inhomogenous indoor climate. An alternative approach to solve these problems is provided by the simulation of the indoor climate with computational fluid dynamics (CFD) in combination with a detailed thermal comfort model describing the human thermoregulation (Cropper et al., 2009; Gao et al., 2009; van Treeck 2009; Voelker et al., 2009b).

There are several options for the data transfer from the CFD to the thermoregulation model. To pass the heat flux q of the human body to the environment to the thermoregulation model, and receiving surface temperatures of the human body in return, cannot be recommended for reasons of numerical stability. A better choice is transmitting the heat transfer coefficient for every single segment based on a fluid reference temperature. This fluid reference temperature can be the air temperature of the undisturbed environment (outside the boundary layer of the human body). As later explained, it is not easy to determine this air temperature for every single segment. Therefore, the so called local heat transfer coefficient and the near-wall temperature, both being provided by the CFD code, can be alternatively used for the calculation of the convective heat losses. In any case, the undisturbed air temperature at every segment is needed, at least for the calculation of the heat losses due to evaporation of sweat as well as respiration. For this purpose, an averaged room air temperature is often used, which is suboptimal when investigating non-uniform environments.

On this account, a comprehensive knowledge of the micro-climate surrounding the human body is necessary for the data transfer from CFD to the thermal comfort model. Resulting from the heat release, the micro-climate surrounds the human body featuring a boundary layer and an ascending plume both differing greatly from the indoor climate. However, the common thermal comfort models usually require the climatic data of the undisturbed indoor environment. Therefore, the climatic parameters have to be retrieved from the CFD simulation far from the skin surface. On the other hand, these parameters have to be picked as close as possible to the corresponding body part, otherwise the approach of determining local thermal comfort is meaningless. On this account, the thickness of the boundary layer has to be known.

Comparing all body segments, the micro-climate can strongly vary in thickness and shape. As investigated by (Murakami et al., 1997), the thickness of the thermal boundary layer surrounding the feet is comparatively small (s_0=5 cm). This layer becomes thicker with increasing height. Large surfaces along the flow direction like chest and back are covered with a relatively thick layer, which is associated with a low convective heat loss. For the neck, a thickness of 19 cm was measured. The thickness of the micro-climate defined by the air flow s_v differs from the thermal boundary layer covering around 8 cm at the feet and about 15 cm at the head (Murakami et al., 1997). The velocity of the ascending air flow has its maximum within the plume above the head with 0,2-0,3 m/s (Murakami 2002).

As own measurements and simulations have shown, the properties of the micro-climate are highly dependent on the boundary conditions and the particular body segment. Under normal conditions, the convective heat transfer of the human body is dominated by buoyancy-driven convection. One of the primary impact factors is the temperature difference between the surface of the human body and the surrounding air. Other parameters including clothing or activity strongly influence the

temperature difference. In addition, the flow velocity is significantly responsible for the convective heat transfer. The higher the flow velocity, the thinner the boundary layer and the higher the heat transfer coefficient. Therefore, the previously mentioned values are not sufficient to define the disturbed area around the human body, which is necessary for the coupling of CFD and a human thermoregulation model. On this account, a simple but practical approach solving this problem is introduced in this paper.

MEASUREMENTS

To validate the CFD simulations, a series of measurements has been carried out in a climate chamber (3 m x 3 m x 2.44 m) equipped with a thermal manikin ("Feelix"). The manikin has been used, because the human body affects the temperature and flow conditions as a source of heat and obstacle (Melikov 2004). The measuring setup features the same geometry and boundary conditions as in the simulation, which enables a direct comparison.

To measure the air temperature, a total number of 25 NTC sensor elements with an accuracy of ±0.1 K were used (Figure 1). To visualize the temperature profile, infrared thermography has been employed. As thermography detects only surfaces temperatures, but not the air temperature, an auxiliary work plane made of cardboard was built in a pattern around the thermal manikin. This allows the visualization of the boundary layer of the thermal manikin looking like a surrounding corona. Furthermore, the temperature can be measured in a whole plane, not only at punctually measuring sensors.

Figure 1: Sensors surrounding the thermal manikin

According to (Cehlin et al., 2002), the influence of such impervious planes on the flow and temperature conditions is negligible, assumed that they are aligned parallel to the flow direction at low flow velocities. Both requests met the executed measurements. Disadvantages of this method can be inaccuracies due to the radiation exchange of the cardboard with the surroundings or heat conduction within the cardboard. To control the thermography measurements, a temperature sensor was sticked on the board surface.

In order to detect the speed of the air flow, the two-dimensional Particle Streak Tracking (PST) was used (Dahms et al., 2007). To visualize the flow, a special generator injects about 200 bubbles per second into the climate chamber. For the compensation of the mass of the bubble skin, the particles are filled with helium, which leads to weight neutrality of the about 3 mm large bubbles and a good tracking behavior. The flow field is uniformly illuminated in a plane by LED. This light is pulsed, resulting in characteristic patterns due to the tracer particle, which are recorded with a high resolution SLR. Finally, the particle velocity is calculated based on the distance of the traces and pulse time of the camera. The advantage of this method is, in contrast to the anemometry, the measurement and visualization of the flow velocity in a plane. In addition, the disturbance of the flow through the measurement setup is low.

To double-check the measurements, additional anemometers with an accuracy of ±1,5 % of the measured value have been used. Due to the instability and turbulence of the flow, statistical fluctuations could be measured. For this reason, the measurements were recorded in a period t=1 h with a sampling interval of t=1 s and then averaged. This makes the measurements comparable to the simulation, since the simulation is using the Reynolds-Averaged-Navier-Stokes equations (RANS) statistically averaging the fluctuations in a steady flow. In the following diagrams, the standard deviation (plotted using error bars) provides information about the measured fluctuation. The flow velocity measured with the PST is shown as an interpolated curve, which averages the velocity in terms of time and space allowing comparisons with the simulation.

SIMULATION

For the simulation, the geometry of the available climate chamber has been chosen (Figure 2). The shape of the manikin is a 3d laser scan of the real thermal manikin in the climate chamber. Hence, the geometry used in CFD is an exact copy of the real conditions in the climate chamber, which allows the comparison and, finally, the validation of the simulations. The numerical methods and boundary conditions of the CFD simulation are provided in Table 1.

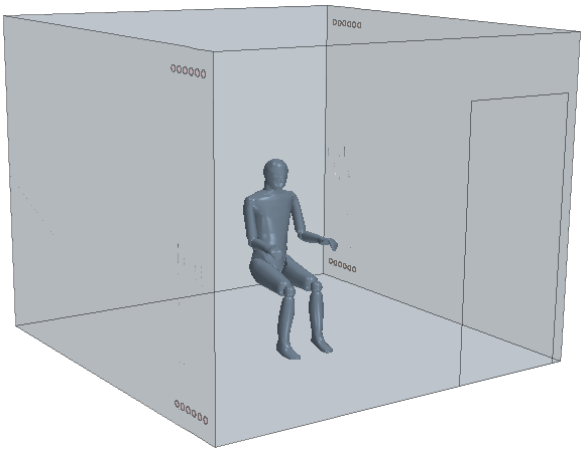

Figure 2: Geometry of the simulated climate chamber

The surface temperature of the manikin was calculated with the UCB Thermal Comfort Model (Huizenga et al., 2001). This model segments the human body into 16 parts. Furthermore, every segment is divided into four concentric layers (core, muscle, fat, skin) plus and additional node for heat and moisture transfer through the clothing (Voelker et al., 2009a). Each single part is represented by its own characteristic parameters. In addition, each layer of every segment is coupled with the centrally operated blood circuit, which is responsible for convective heat transfer.

Table 1
Numerical methods

Model	StarCCM+ (CD-adapco 2010) Turbulence models low-Reynolds k-ε , k-ω SST and V2F (all with standard properties) All y+ wall treatment
Fluid	Air (standard properties, incompressible)
Walls	Wall with defined surface temperature θ_s
Mesh	Polyhedral (~1.600.000 cells), Base size 0.07 m; local refinement 25 % Near wall prism layers, y^+~1
Manikin	Surface temperature of the segments according to the UCBerkeley Thermal Comfort Model

The outcome of this is a system of linked non-linear differential equations indicating the heat balance of the human body. Based on the simulated temperature distribution of the human body, the UCB model is able to determine thermal comfort as well as thermal sensation, both globally and locally. Because of the degree of detail it is possible to determine the effects of inhomogeneous conditions, for example resulting from temperature stratifications or asymmetric radiation.

VALIDATION

The selection of the turbulence model has decisive influence on the outcome of the simulation. For this reason, the results of the turbulence models (1) low-Reynolds k-ε (Lien et al., 1996), (2) V2F (Davidson et al., 2003) and (3) k-ω-SST (Menter 1994) have been compared with measurements. The aim is the selection of the most appropriate turbulence model for this application.

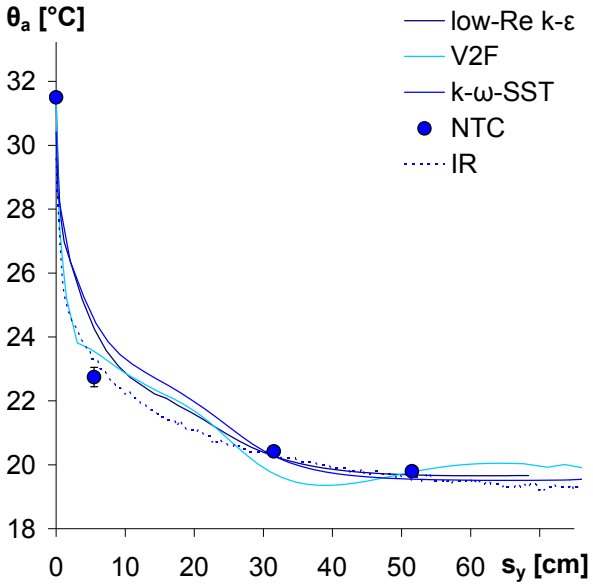

Figure 3: Air temperature vertically above the shoulder (s_y=0 is at the surface of the shoulder)

For the validation, wall surface temperatures were set to be 18°C. Due to the heat loss of the manikin, the room temperature is slightly above this value. Considering the measurement error, a good agreement with the simulation could be found. As an example serves Figure 3 with a comparison of the simulated air temperature of all turbulence models plus the measurements with NTC sensors and thermography. The same applies for Figure 4, where the air velocity above the head was measured and compared to the simulation.

The detailed examination at various positions reveals that the k-ω-SST model best matches the measurements. The reason might be the implemented blending function that uses the k-ε model within the free space but near the wall the k-ω model, combining the advantages of both models.

For this reason, all subsequent simulations were carried out with this turbulence model. Further studies have been carried out to ensure that the k-ω-SST model also allows reliable predictions with different boundary conditions (Voelker et al., 2011b; Voelker et al., 2011a).

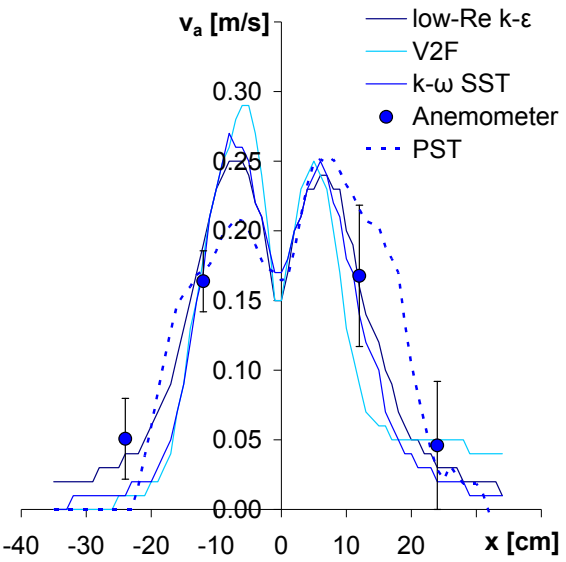

Figure 4: Air velocity 3 cm horizontally above the head (x=0 is the symmetry plane of the manikin)

However, the thermographic measurements show some weak points, as they differ from the NTC measurements and the simulation. Reason is the radiation exchange with the surroundings plus the reflection of the walls during the recording of the thermogram. In summary, it can be seen that the simulations carried out under different conditions show a good agreement with the measurements. Minor inaccuracies can be explained and are due to the fact that both measurement and simulation are only an approximation of reality.

RESULTS

The air temperature and flow velocity of the micro-climate was simulated for various boundary conditions. In Figure 5 and Figure 6, the results are visualized for a uniform wall temperature θ_w=18°C. Due to the heat release of the human via convection and conduction, the micro-climate shows temperatures inbetween the room air temperature and the surface temperature of the manikin. This temperature gradient is responsible for a density gradient, which is in case of natural convection the reason for the mass transport.

While the thermal micro-climate is very thin in the area of the lower torso, it expands with increasing altitude. Especially the changing geometry of the body at the neck leads to an expansion. In this area, the highest air temperatures are to be found. The cause of the hot spots at the shoulders is the reduced heat transport due to warm air rising from the lower body. In addition, the head is a barrier for the thermal buoyancy. At the head, a relatively thick thermal layer can be found, which results in an ascending plume.

When investigating the flow velocity (Figure 6), similar but not identical properties can be seen. Very close to the human body, the shear stress is slowing the velocity. In the boundary layer, an air velocity of about 0.1 m/s can be found. As the thermal micro-climate, the air flow expands significantly at the neck. At the head and above, the flow velocity has its maximum with a velocity slightly higher than 0.3 m/s.

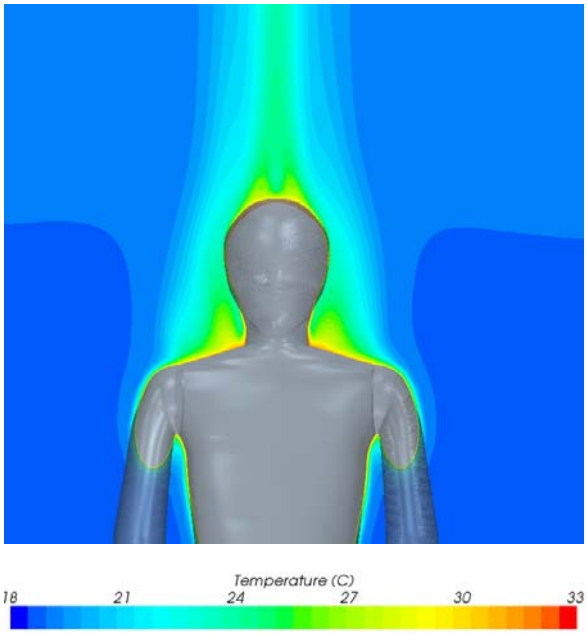

Figure 5: Simulated air temperature in the micro-climate

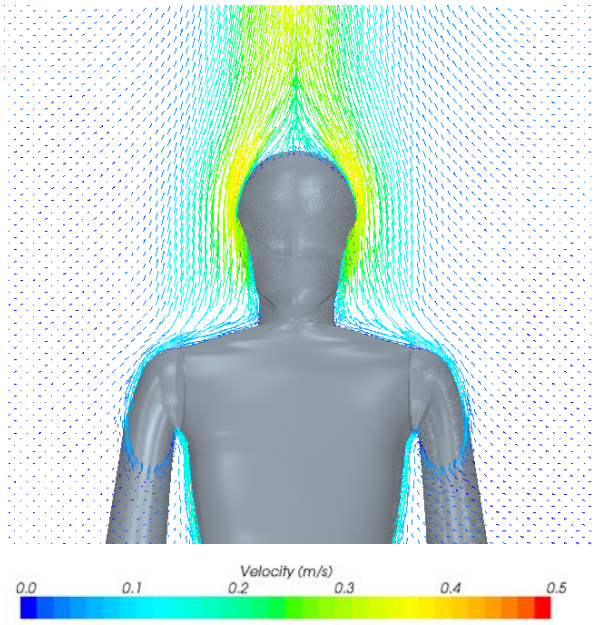

Figure 6: Simulated air velocity in the micro-climate

Striking is a so-called dead zone directly above the head. The break-off point of the flow is behind the maximum thickness of the head (supercritical flow), which is a result of the high Reynolds and Grashof numbers respectivly the turbulent flow in this region.

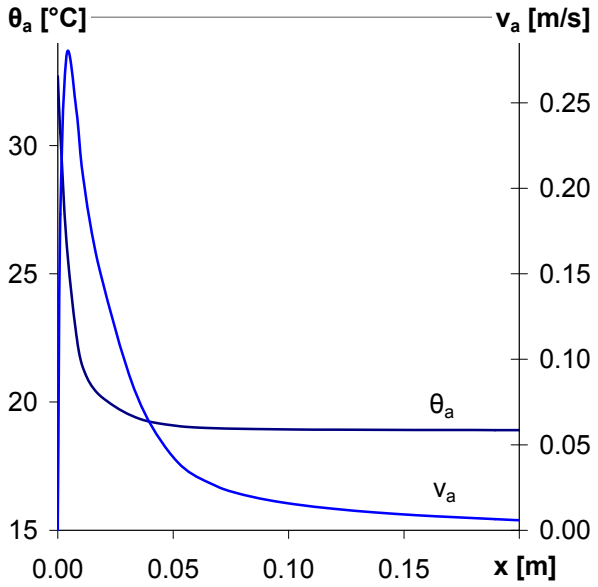

Figure 7: Simulated air temperature and velocity of the micro-climate, with increasing distance from the head at θ_a = 18°C

A detailed overview about the differences between the thermal boundary layer s_θ and the layer defined by the air flow s_v provides Figure 7. The air temperature decreases with increasing distance from the body until it reaches the value of the undisturbed air temperature. Contrary, the flow velocity at the surface is zero due to the shear stress, but increases in the micro-climate with increasing distance. After reaching a maximum, it falls to the value of the undisturbed air velocity (in case of buoyancy-driven convection). The reason of the unequal thickness is the Prandtl number, which is the ratio of the thickness of the flow and the thermal boundary layer (Pr_{Luft} ~ 0.7).

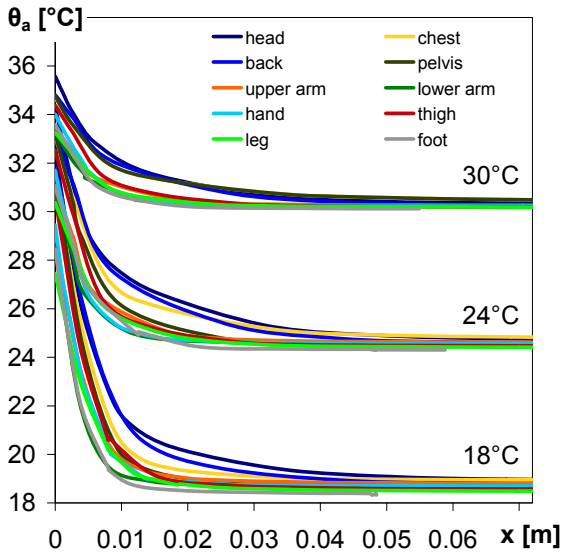

Figure 8: Simulated air temperature with increasing distance from the body parts at various boundary conditions

As discussed in the introduction of this paper, the thermal comfort model requires the climatic parameters of the undisturbed indoor climate. As the thickness of the micro-climate depends on the boundary conditions (Figure 8), generalized values of the thickness of the micro-climate do not help.

To retrieve the undisturbed air temperature automatically out of the CFD simulation, the following approach has been chosen. The air temperature is taken orthogonally to the body surface for each cell of the CFD simulation. Then an algorithm determines the undisturbed air temperature based on the temperature curve. On the basis of the difference between predecessor and successor

$$\varepsilon \geq \theta_a(x_{i-1}) - \theta_a(x_i), \qquad (1)$$

a stopping criterion (e.g. 0.01 K/m) has to be defined (Figure 9). A disadvantage is that any irregularities in the course of the temperature due to numerical inaccuracies can result in a false value. To increase the accuracy other predecessors may be included into this approach.

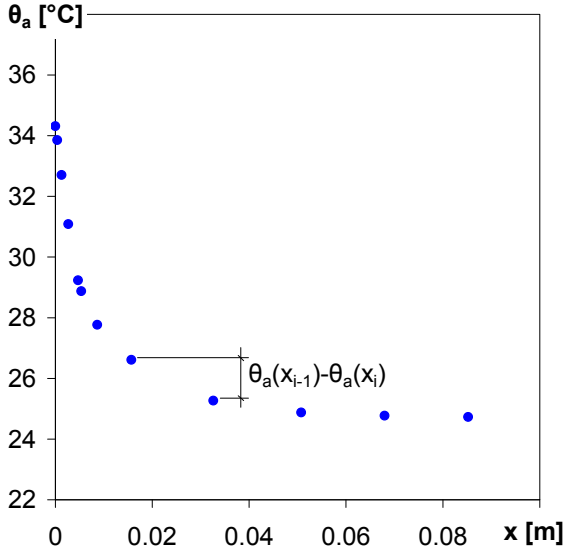

Figure 9: Simulated air temperature with increasing distance from the body surface at 24°C

As this is still fraught with uncertainty, the approximation of a function from the simulated values is recommended. Investigations of the simulated air temperature in the micro-climate at all segments under different conditions showed that the exponential equation

$$\theta_a(x) = a + b \cdot e^{cx} \qquad (2)$$

leads to a very good match (R^2=0.995; σ=0.01) especially in the crucial area of the transition from the micro-climate to the undisturbed air temperature. The determination of the coefficients a, b and c is

done for each boundary condition and for each segment based on the method of least squares. With the derivative of this function, the point of the curve is determined at which the slope is equal to the stopping criterion

$$\theta_a^{'}(x) \leq \varepsilon \,. \qquad (3)$$

Both methods introduced are rather independent of the boundary conditions and thus, in contrast to the previous approaches, generally applicable.

Besides the air temperature, the air velocity has to be transferred in the majority of cases when coupling CFD and thermal comfort models. The background is the need of the determination of the convective heat transfer coefficients, for examples basing on the measurements of (de Dear et al., 1997).

However, the conditions of the experiments can be hardly generalized and transferred to other boundary conditions, as own measurements and simulations show. For this reason, the heat transfer coefficients are determined directly in the CFD simulation based on

$$h_c = \frac{q}{\theta_s - \theta_a} \,. \qquad (4)$$

While the heat flux q is known from the CFD simulation (Figure 10), the air temperature has been already assessed by equation (1) and (2). Alternatively, the (local) heat transfer coefficient can be determined with the temperature of the near-wall cell. In this case, the near-wall temperature has to be sent to the thermoregulation model to calculate the convective heat losses.

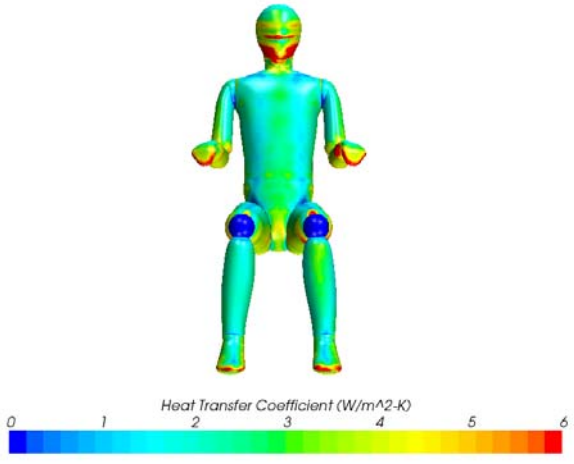

Figure 10: Simulated convective heat transfer coefficient at 24°C

CONCLUSION

A climate chamber equipped with a thermal manikin has been used to validate CFD simulations against measurements for different boundary conditions. The simulations using the k-ω-SST turbulence model show the best agreement with the measurements. Based on the validation, CFD has been used to gain knowledge about the micro-climate surrounding the human body. The simulations show, that the micro-climate largely depends on the boundary conditions and on the particular body segement. Therefore, generalized values describing the thickness of the micro-climate cannot be used for the data exchange between CFD and the thermal comfort model. Finally, the findings have been used to develop an approach for the automeated data exchange including air temperature and heat transfer coefficient.

ACKNOWLEDGEMENT

This paper forms part of our work in the research project “Methoden und Baustoffe zur nutzer-orientierten Bausanierung”, which is funded by the German Federal Ministry for Education and Research (BMBF) and administrated by Projektträger Jülich. Additionally we highly appreciate the cooperation with the Center for the Built Environment, UC Berkeley.

REFERENCES

CD-adapco 2010. *STAR-CCM+. Version 5.02.009*.

Cehlin, M., Moshfegh, B. & Sandberg, M. 2002. Measurements of air temperatures close to a low-velocity diffuser in displacement ventilation using an infrared camera. Energy and Buildings 34 (7): 687-698.

Cropper, P. C., Yang, T., Cook, M. J., Fiala, D. & Yousaf, R. 2009. Coupling a human thermal comfort model with computational fluid dynamics to predict thermal comfort in naturally ventilated environments. Journal of Building Performance Simulation 3 (3): 233-243.

Dahms, A., Rank, R. & Müller, D. 2007. Enhanced Particle Streak Tracking system (PST) for two dimensional airflow pattern measurements in large planes. Roomvent, Helsinki, Finland.

Davidson, L., Nielsen, P. V. & Sveningsson, A. 2003. Modifications of the v2f model for computing the flow in a 3D wall jet. Turbulence, Heat and Mass Transfer (4): 577-584.

de Dear, R. J., Arens, E., Hui, Z. & Oguro, M. 1997. Convective and radiative heat transfer coefficients for individual human body segments. International Journal of Biometeorology 40 (3): 141-156.

Gao, N. P., Niu, J. & Zhang, H. 2009. Coupling outer-body airflow and inner-body thermoregulation models to predict thermal comfort in nonuniform environments. Building Simulation, Glasgow, Scotland.

Huizenga, C., Zhang, H. & Arens, E. 2001. A model of human physiology and comfort for assessing

complex thermal environments. Building and Environment 36 (6): 691-699.

Lien, F. S., Chen, W. L. & Leschziner, M. A. 1996. Low-Reynoldsnumber eddy-viscosity modelling based on non-linear stress-strain/vorticity relations. Symposium on Engineering Turbulence Modelling and Measurements, Crete, Greece.

Melikov, A. 2004. Breathing thermal manikins for indoor environment: important characteristics and requirements. European Journal of Applied Physiology 92 (6): 710-713.

Menter, F. R. 1994. Two-Equation Eddy-Viscosity Turbulence Models for Engineering Applications. AIAA Journal 32 (8): 1598-1605.

Murakami, S. 2002. CFD study on the micro-climate around the human body with inhalation and exhalation. Roomvent, Copenhagen, Denmark.

Murakami, S., Kato, S. & Zeng, J. 1997. Flow and temperature fields around human body with various room air distribution. CFD study on computational thermal manikin - Part 1. ASHRAE Transactions 103 (1): 3-15.

van Treeck, C. 2009. Model-adaptive analysis of indoor thermal comfort. Building Simulation, Glasgow, Scotland.

Voelker, C., Hoffmann, S., Kornadt, O., Arens, E., Zhang, H. & Huizenga, C. 2009a. Heat and moisture transfer through clothing. Building Simulation, Glasgow, Scotland.

Voelker, C. & Kornadt, O. 2011a. Simulation and measurement of thermal comfort and sensation. Indoor Air, Austin (Tx), USA.

Voelker, C. & Kornadt, O. 2011b. Thermal comfort – simulation and measurement using a thermal manikin. Roomvent, Trondheim, Norway.

Voelker, C., Kornadt, O., Zhang, H. & Arens, E. 2009b. Thermal comfort in rooms with radiant cooling. Roomvent, Busan, South Korea.